Journal of Organometallic Chemistry 693 (2008) 3627–3637

Contents lists available at ScienceDirect

Journal of Organometallic Chemistry

journal homepage: www.elsevier.com/locate/jorganchem

Quantum chemical study of ethylene addition to group-7 oxo complexes $MO_2(CH_3)(CH_2)$ (M = Mn, Tc, Re) ☆

Robin Haunschild, Gernot Frenking *

Fachbereich Chemie der Philipps-Universität Marburg, Hans-Meerwein-Straße, 35043 Marburg, Germany

ARTICLE INFO

Article history:
Received 12 June 2008
Received in revised form 28 August 2008
Accepted 2 September 2008
Available online 10 September 2008

Keywords:
Metal oxo complexes
Reaction mechanism
DFT calculations

ABSTRACT

Quantum chemical calculations using DFT at the B3LYP level have been carried out for the reaction of ethylene with the group-7 compounds $ReO_2(CH_3)(CH_2)$ (**Re1**), $TcO_2(CH_3)(CH_2)$ (**Tc1**) and $MnO_2(CH_3)$- (CH_2) (**Mn1**). The calculations suggest rather complex scenarios with numerous pathways, where the initial compounds **Re1**–**Mn1** may either engage in cycloaddition reactions or numerous addition reactions with concomitant hydrogen migration. There are also energetically low-lying rearrangements of the starting compounds to isomers which may react with ethylene yielding further products. The $[2 + 2]_{Re,C}$ cycloaddition reaction of the starting molecule **Re1** is kinetically and thermodynamically favored over the $[3 + 2]_{C,O}$ and $[3 + 2]_{O,O}$ cycloadditions. However, the reaction which leads to the most stable product takes place with initial rearrangement to the dioxohydridometallacyclopropane isomer **Re1a** that adds ethylene with concomitant hydrogen migration yielding **Re1a**-**1**. The latter reaction has a slightly higher barrier than the $[2 + 2]_{Re,C}$ cycloaddition reaction. The direct $[3 + 2]_{C,O}$ cycloaddition becomes more favorable than the $[2 + 2]_{M,C}$ reaction for the starting compounds **Tc1** and **Mn1** of the lighter metals technetium and manganese but the calculations predict that other reactions are kinetically and thermodynamically more favorable than the cycloadditions. The reactions with the lowest activation barriers lead after rearrangement to the ethyl substituted dioxometallacyclopropanes **Tc1a**-**1** and **Mn1a**-**1**. The manganese compound exhibits an even more complex reaction scenario than the technetium compounds. The thermodynamically most stable final product of ethylene addition to **Mn1** is the ethoxy substituted metallacyclopropane **Mn1a**-**2** which has, however, a high activation barrier.

1. Introduction

Numerous quantum chemical studies have shown that the initial step of the olefin addition to OsO_4 is a concerted [3 + 2] reaction yielding an osma-2,5-dioxolane as an intermediate [1] rather than an [2 + 2] cycloaddition of the olefin with OsO_4 and a subsequent rearrangement of the resulting osmaoxetane. Consecutively, the intermediate eliminates the *cis*-dihydroxylated olefin. The [3 + 2] addition is more favorable because it has a significantly lower barrier than the [2 + 2] one. Further quantum chemical investigations [2] concluded that RuO_4, ReO_3^- and similar metal oxides also prefer a [3 + 2] cycloaddition pathway over a [2 + 2] one [3]. The presence of an imido group does not change the reactivity significantly. Deubel and Muñiz found that a [3 + 2] cycloaddition pathway is still preferred for $Os(NH_2)_2O_2$ rather than the [2 + 2] one [4]. The authors predicted a decrease of the activation energies in the order O/O > O/NH > NH/NH.

This situation changes when a transition metal–carbon double bond is present: the [2 + 2] cycloaddition across the carbon–metal bond becomes competitive for the ethylene addition to $OsO_3(CH_2)$ and $OsO_2(CH_2)_2$ [5–7]. For $ReO_2(CH_3)(CH_2)$ and $WO(CH_3)_2(CH_2)$, it becomes even more favorable than the possible [3 + 2] [7,8] cycloaddition pathways. Exchanging the transition metal tungsten by molybdenum or chromium, the preference of a [2 + 2] cycloaddition across the transition metal–carbon double bond over an alternative [3 + 2] one does not change significantly [9]. We extended our quantum chemical studies of the group-7 elements. In this paper, we present our theoretical results of the reaction pathways for the ethylene addition to $ReO_2(CH_3)(CH_2)$, $TcO_2(CH_3)(CH_2)$ and $MnO_2(CH_3)(CH_2)$. A subset of the presented reaction pathways for the direct ethylene addition to $ReO_2(CH_3)(CH_2)$ (**Re1**) was already published in Ref. [7]. Our calculations are restricted to molecules in the singlet electronic state. Therefore, we cannot exclude that higher spin states may play a role in the reactions, but the present work gives an overview of the possible reaction pathways for the rhenium, technetium and manganese compounds in the singlet state.

☆ R. Haunschild, G. Frenking, Theoretical studies of organometallic compounds. 59. Part 58, J. Organomet. Chem. 693 (2008) 737.

* Corresponding author. Tel.: +49 6421 2825563; fax: +49 6421 2825566.
E-mail address: Frenking@chemie.uni-marburg.de (G. Frenking).

0022-328X/$ - see front matter © 2008 Elsevier B.V. All rights reserved.
doi:10.1016/j.jorganchem.2008.09.007

2. Methods

All geometry optimizations were carried out using gradient corrected density functional theory (DFT) employing the B3LYP hybrid functional [10] as implemented [11] in the GAUSSIAN 03 program [12] without any symmetry constraints. Ahlrich's triple zeta basis set (TZVP) [13] was used for the elements O, C and H. For the transition metals, the Stuttgart/Köln relativistic effective pseudo potentials (ECP) replacing 60 (for rhenium), respectively 28 (for technetium) and 10 (for manganese) core electrons was employed in combination with a (311111/22111/411) (for rhenium and technetium) [14], respectively (311111/22111/411/1) (for manganese) [15] valence basis set. This combination is denoted as basis set I. Analytical vibrational harmonic frequencies were calculated at all stationary points to verify their nature (minimum, transition state or higher order saddlepoint). Intrinsic reaction coordinate (IRC) [16] calculations were carried out to ensure the connectivity of the minima and transition states. For transition states with an imaginary mode of too small magnitude, dynamic reaction path (DRP) [17] calculations were done instead. The DRP calculations were carried out using the frog module of the TURBOMOLE program [18]. Here, a slightly different valence basis set for the transition metals was employed: for rhenium, a (211111/411/311) and for technetium, a (31111/411/311) valence basis set was used in conjunction with the Stuttgart/Köln ECPs, whereas for manganese, no ECP was employed. Instead Ahlrich's all-electron triple zeta basis set (842111/6311/411) [19] was used. Additional B3LYP single point energies were computed at all transition states and minima with a larger basis set denoted as basis set II. There, the correlation consistent triple zeta basis sets of Dunning (cc-pVTZ) [20] were used for the elements O, C and H. The transition metal basis set is augmented by two sets of f and one set of g functions derived by Martin and Sundermann [21]. All energies discussed in this study relate to B3LYP/II//B3LYP/I and are corrected by the unscaled zero point energy (ZPE) contributions obtained at B3LYP/I unless or otherwise stated.

3. Results and discussion

The presentation of the results is organized as follows. For each metal parent compound $MO_2(CH_3)(CH_2)$ (**M1**) we first present the calculated reaction profiles for intramolecular rearrangement to other isomers **M1a**–**M1h**. As the next step we give the reaction coordinates for ethylene addition to the energetically lowest lying isomers which are expected to play a role in the thermal addition reaction. Reaction pathways for ethylene addition of high-lying isomers of **M1** have not been considered. The reaction types are divided into cycloadditions ([1 + 2], [2 + 2], [3 + 2]) and addition reactions with concomitant hydrogen migration.

3.1. Reactions of $ReO_2(CH_3)(CH_2)$

Eight isomeric forms **Re1a**–**Re1h** were found as minima on the potential energy surface (PES) besides the parent compound **Re1**. On the left-hand-side of Fig. 1 three rearrangements leading to cyclic isomers (**Re1a**, **Re1b** and **Re1d**) are shown, while five isomerizations yielding acyclic structures are presented on the right hand side. Six of them are directly connected to **Re1** by a single transition state, whereas **Re1c** and **Re1f** are accessible via two-step pathways. However, the second step of the rearrangement **Re1** → **Re1e** → **Re1f** has a negligible barrier which completely disappears after ZPE corrections are made. Therefore, it seems unlikely that **Re1e** can be isolated. For **Re1a**, we found both: a direct transition state from **Re1** (on the left hand side) and a two-step rearrangement (**Re1** → **Re1e** → **Re1a**, on the right hand side). The latter is much more favorable than the former because the overall barrier for the two-step rearrangement (30.3 kcal/mol) is by far lower than the direct one (83.0 kcal/mol). The cyclic species **Re1a** is the only isomer which is lower in energy than the parent compound **Re1**, but the rearrangement is exothermic by only 5.2 kcal/mol. **Re1f** is nearly degenerate with **Re1**. The calculations indicate that **Re1** lies in a rather deep potential well; only the isomerization **Re1** → **Re1e** with subsequent rearrangements to **Re1a** and **Re1f** should play a role under thermal conditions. Therefore, we calculated the reaction profiles for the ethylene addition to **Re1**, **Re1a** and **Re1f**. Fig. 2 shows the results for the reaction **Re1** + C_2H_4. The geometries of the most important minima and transition states are shown in Fig. 1S of Supplementary material.

Numerous reaction pathways for concerted [3 + 2], [2 + 2] and [1 + 2] cycloadditions have been found for the reaction **Re1** + C_2H_4 which are shown on the right hand side of Fig. 2. The $[2 + 2]_{Re,C}$

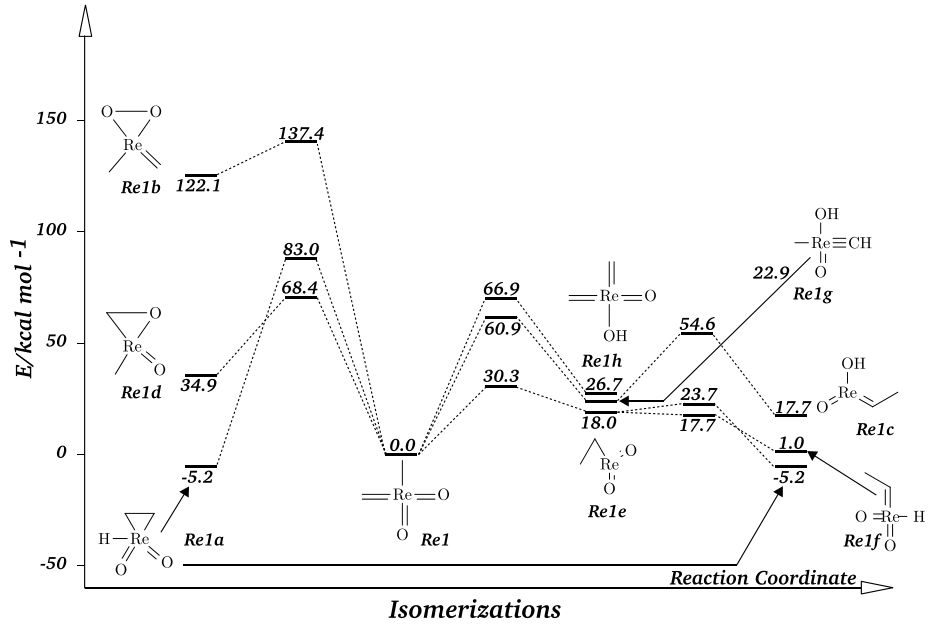

Fig. 1. Calculated reaction profile for the isomerizations of $(O=)_2Re(CH_3)(=CH_2)$ (**Re1**) at B3LYP/II//B3LYP/I+ZPE.

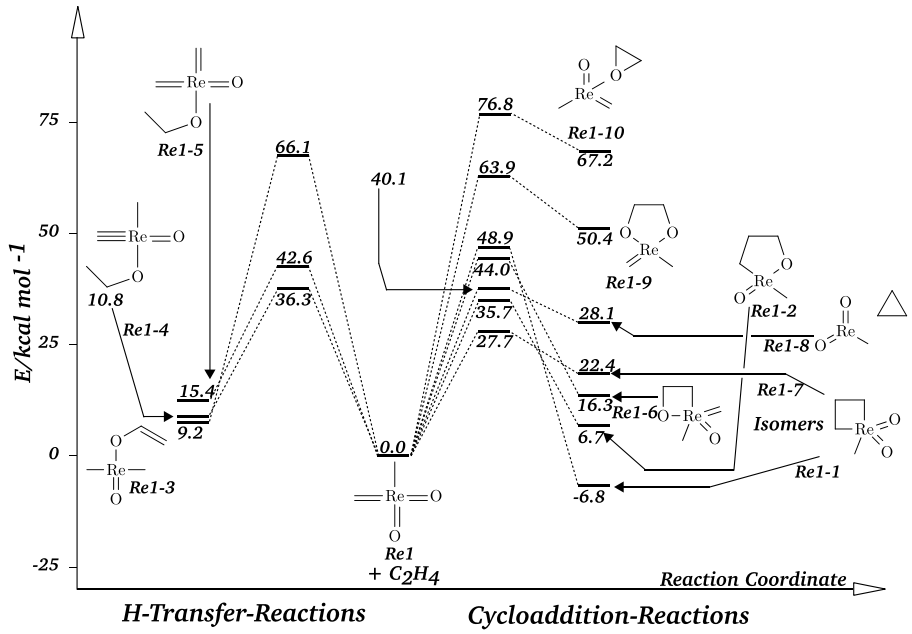

Fig. 2. Calculated reaction profile for the ethylene addition to $(O{=})_2Re(CH_3)({=}CH_2)$ (**Re1** + C_2H_4) at B3LYP/II//B3LYP/I+ZPE.

cycloaddition across the rhenium–carbon double bond is the *only* exothermic addition reaction of **Re1** yielding **Re1-1**, but it has a rather high activation barrier of 48.9 kcal/mol. The exothermicity is also quite low with −6.8 kcal/mol. There are two isomers of the rhenacyclobutane, structures **Re1-1** and **Re1-7**. The latter species has a distorted trigonal bipyramidal structure with the oxo ligands in the axial positions and the carbon substituents in the equatorial place. The structure of the much more stable isomer **Re1-1** is best described by a distorted square pyramid. The latter isomer is 29.2 kcal/mol higher in energy than the former but the activation barrier for the $[2+2]_{Re,C}$ addition yielding **Re1-7** (27.7 kcal/mol) is much lower than the activation energy which yields **Re1-1**. There is no pathway for the direct interconversion between **Re1-1** and **Re1-7**. Small changes of the geometry of **Re1-7** give rise to ethylene dissociation since the activation barrier **Re1-7** → **Re1** + C_2H_4 is very low. An opposed result was previously found for the $[2+2]_{M,C}$ addition of ethylene to the group-6 compounds $MO(CH_3)_2(CH_2)$ (M = Cr, Mo, W) [9]. There, an interconversion between the two $[2+2]_{M,C}$ products was found in contrast to the present study. The calculations thus give the rather curious result that the two $[2+2]_{Re,C}$ addition reactions yielding the rhenacyclobutane isomers **Re1-1** and **Re1-7** are the thermodynamically (**Re1-1**) and kinetically (**Re1-7**) most favored reactions of **Re1** + C_2H_4. All other reactions have higher barriers or are more endothermic (Fig. 2). In particular, we want to point out that the $[3+2]_{C,O}$ cycloaddition reaction yielding **Re1-2** and the $[3+2]_{O,O}$ addition yielding **Re1-9** are less favored than the $[2+2]_{Re,C}$ addition. The $[2+2]_{Re,O}$ addition **Re1** + C_2H_4 → **Re1-6** is kinetically and thermodynamically also more favorable than the $[3+2]_{O,O}$ addition but it has a higher barrier and is more endothermic than the $[3+2]_{C,O}$ addition. The $[1+2]_O$ addition yielding the energetically high-lying product **Re1-10** is the least favorable reaction. The endothermic $[1+2]_C$ addition is more favorable but still has an activation barrier of 40.1 kcal/mol. In the latter reaction dissociation takes place yielding cyclopropane and $MeReO_2$ as products.

On the left hand side of Fig. 2 three reaction courses are shown, where a hydrogen migration takes place. All reactions are endothermic. In the reactions **Re1** + C_2H_4 → **Re1-4** and **Re1** + C_2H_4 → **Re1-5**, one hydrogen atom migrates from **Re1** to ethylene while in the process **Re1** + C_2H_4 → **Re1-3** the hydrogen atom moves in the opposite direction. The high barriers and the endothermicity suggest that the latter reactions should not play a role in the thermal ethylene addition to **Re1**. Overall, the latter parent system should not be very reactive for ethylene addition since the only exothermic reaction yielding **Re1-1** has a high barrier of 48.9 kcal/mol. The search for a structure where ethylene directly binds to the rhenium atom of **Re1** did not yield a minimum on the PES.

Next we discuss the reaction profile for ethylene addition to the isomer **Re1a** which is 5.2 kcal/mol more stable than the parent system **Re1**. The theoretically predicted pathways are shown in Fig. 3.

On the right hand side pathways for $[3+2]_{O,O}$, $[2+2]_{Re,O}$ and $[1+2]_O$ ethylene addition to **Re1a** are shown. The $[2+2]_{Re,O}$ addition across the Re═O double bond yielding **Re1a-3** is kinetically and thermodynamically clearly favored over the $[3+2]_{O,O}$ addition **Re1a** + C_2H_4 → **Re1a-4**. Both reactions are endothermic and have rather high activation barriers. The $[1+2]_O$ addition has also a high activation barrier leading to the energetically high-lying product **Re1a-5**. A low activation barrier of 11.1 kcal/mol has been found for the degenerate ethylene exchange reaction which is shown on the left hand side of Fig. 3. The only exothermic reaction which has a comparatively low activation barrier of 24.4 kcal/mol is the ethylene addition to the rhenium atom with simultaneous hydrogen migration **Re1a** + C_2H_4 → **Re1a-1**. The latter product may rearrange to the isomers **Re1a-1a** and **Re1a-1b** but the activation barriers for the endothermic reactions are very high. The addition reaction of ethylene to the oxygen atom of **Re1a** with concurrent hydrogen migration yielding **Re1a-2** has a very high activation barrier.

The remaining low-energy isomer of **Re1** which needs to be considered for the reaction with ethylene is **Re1f**. Fig. 4 shows the theoretically predicted reaction pathways.

We found altogether seven pathways for [3 + 2], [2 + 2] and [1 + 2] addition reactions of the system **Re1f** + C_2H_4. They are shown on the right hand side of Fig. 4. All cycloaddition reactions have barriers of >30 kcal/mol and only the $[2+2]_{Re,C}$ addition yielding **Re1f-1** is a slightly exothermic reaction. The latter structure has again an energetically much higher lying form **Re1f-7** but the activation barrier **Re1f** + C_2H_4 → **Re1f-7** is clearly lower

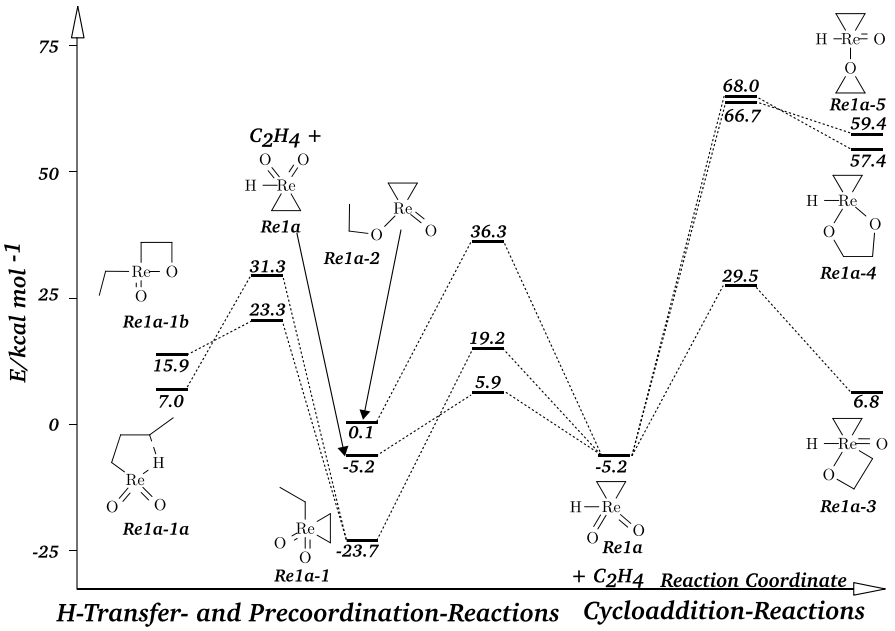

Fig. 3. Calculated reaction profile for the ethylene addition to $(O=)_2Re(CH_2CH_2)(H)$ (**Re1a** + C_2H_4) at B3LYP/II//B3LYP/I+ZPE.

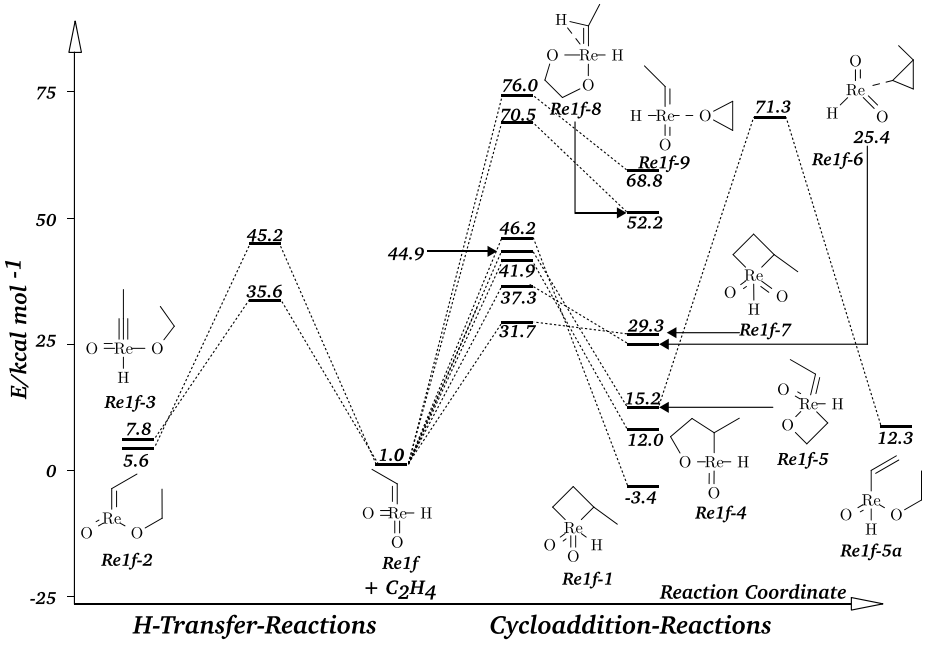

Fig. 4. Calculated reaction profile for the ethylene addition to $(O=)_2Re(CHCH_3)(H)$ (**Re1f** + C_2H_4) at B3LYP/II//B3LYP/I+ZPE.

(31.7 kcal/mol) than the barrier for **Re1f** + C_2H_4 → **Re1f-1** (46.2 kcal/mol). The situation is thus similar to the above discussed $[2+2]_{Re,C}$ addition of the parent structure **Re1**. The $[3+2]_{O,O}$ addition has a very large barrier (70.5 kcal/mol) and it is endothermic by 52.2 kcal/mol. The $[3+2]_{C,O}$ reaction has a lower barrier (41.9 kcal/mol) and is much less endothermic (12.0 kcal/mol) but it cannot compete with the $[2+2]_{Re,C}$ reaction. The left hand side of Fig. 4 shows the pathways for two addition reactions with simultaneous hydrogen migrations. Both reactions are slightly endothermic and have rather higher barriers. None of the reactions shown in Fig. 4 should play a role in the thermal addition of ethylene to **Re1**.

In summary, the kinetically most favorable reaction of **Re1** with ethylene is the direct $[2+2]_{Re,C}$ cycloaddition yielding the energetically high-lying species **Re1-7** in a reaction which is endothermic by 22.4 kcal/mol. The reaction has an activation barrier of 27.7 kcal/mol. The $[3+2]_{C,O}$ cycloaddition yielding **Re1-2** has a clearly higher barrier of 35.7 kcal/mol. The most exothermic reaction takes place after rearrangement of the slightly more stable isomer **Re1** → **Re1a** and subsequent addition with concurrent hydrogen migration yielding the dioxorhenacyclopropane species **Re1a-1**. The latter reaction has an overall barrier of 30.3 kcal/mol which comes from the rearrangement step and it is exothermic by 23.7 kcal/mol.

3.2. Reactions of $TcO_2(CH_3)(CH_2)$

Fig. 5 shows the reaction pathways for the rearrangements of the parent technetium compound $TcO_2(CH_3)(CH_2)$ (**Tc1**) to other isomers. The equilibrium structures **Tc1a**–**Tc1h** are analogous to the eight rhenium species which are shown in Fig. 1. A comparison of the reaction profiles for the technetium compounds with the rhenium species shows that the activation barrier for the formation of the Tc compound is always lower than for the respective Re molecule and that the former reactions are thermodynamically more favored than the latter. There are now two isomers which are lower in energy than **Tc1**. The most stable form is **Tc1a** which is 12.5 kcal/mol lower in energy than **Tc1** while the isomer **Tc1f** is only 1.5 kcal/mol more stable than **Tc1**. The activation barrier **Tc1** → **Tc1a** is 22.9 kcal/mol. The isomer **Tc1f** is not accessible via direct rearrangement from **Tc1** but only via consecutive hydrogen transfer reaction **Tc1a** → **Tc1f** which has an activation energy of 27.7 kcal/mol. All other isomeric forms of **Tc1** are energetically higher lying and have very high activation barriers. Therefore, we consider only the ethylene addition reactions to **Tc1**, **Tc1a** and **Tc1f**. The reaction pathways of **Tc1** are shown in Fig. 6. The geometries of the most important minima and transition states are shown in Fig. 2S of Supplementary material.

Like for the rhenium compound **Re1**, seven cycloaddition pathways for $[3+2]_{,}$ $[2+2]$ and $[1+2]$ additions of ethylene are found for **Tc1** which are shown on the right hand side of Fig. 6. In contrast to the rhenium homologue, the $[2+2]_{M,C}$ cycloaddition across the M=CH_2 double bond is not the thermodynamically preferred pathway. For the technetium system, the $[3+2]_{C,O}$ cycloaddition **Tc1** + C_2H_4 → **Tc1-1** is slightly more exothermic (ΔE_R = −10.4 kcal/mol) than the $[2+2]_{Tc,C}$ reaction yielding **Tc1-3** (ΔE_R = −8.0 kcal/mol) and also the activation barrier of the former reaction (ΔE_A = 27.5 kcal/mol) is lower than for the latter (ΔE_A = 49.4 kcal/mol). The preference for a [3 + 2] reaction over a [2 + 2] reaction may thus depend on the nature of the metal! For the $[2+2]_{Tc,C}$ reaction we found again two strikingly different pathways which lead to two isomeric forms of the metallacyclobutane **Tc1-3** and **Tc1-8**. The pathway yielding the significantly less stable **Tc1-8** has a much lower barrier (ΔE_A = 28.5 kcal/mol) than the addition reaction leading to **Tc1-3** (ΔE_A = 49.4 kcal/mol). Although the activation barriers for the seven cycloaddition reactions of the technetium compound **Tc1** (Fig. 6) are somewhat lower than those of the rhenium compounds (Fig. 2) they are still too high to become important for a thermal reaction. The lowest activation barrier for the addition of ethylene to **Tc1** is calculated for the $[1+2]_C$ cyclopropanation reaction (26.8 kcal/mol). The activation barriers for the three ethylene additions with concomitant hydrogen migration have even higher barriers of >30 kcal/mol. They are shown on the left hand side of Fig. 6.

Fig. 7 shows the calculated pathways for the system **Tc1a** + C_2H_4 which have a similar feature as the system **Re1a** + C_2H_4 which is shown in Fig. 3. The $[3+2]_{O,O,}$ $[2+2]_{Tc,O}$ and $[1+2]_O$ addition reactions which are shown on the right hand side have rather higher barriers and should not play a role for the actual reaction. Like for the rhenium system, the lowest barrier of 16.7 kcal/mol is predicted for the degenerate ethylene exchange reaction. The thermodynamically most favorable reaction leading to a new product which has also the lowest barrier is the $[1+2]_{Tc}$ ethylene addition to the metal atom **Tc1a** + C_2H_4 → **Tc1a-1**. The activation barrier is 19.2 kcal/mol and the reaction is exothermic by 18.1 kcal/mol. The addition with simultaneous hydrogen migration of ethylene to the oxygen atom **Tc1a** + C_2H_4 → **Tc1a-2** is also slightly exothermic by 6.4 kcal/mol but the activation barrier (ΔE_A = 33.4 kcal/mol) is much higher than for the former reaction.

Fig. 8 displays the reaction pathways for ethylene addition to the isomer **Tc1f**. Nine different pathways for cycloaddition reactions and for ethylene addition with concurrent hydrogen migration have been found, but all of them have rather high activation barriers. The kinetically most favorable reaction **Tc1f** + C_2H_4 → **Tc1f-6** has a barrier of 29.7 kcal/mol and it is endothermic by 10.6 kcal/mol. The most exothermic reactions yielding **Tc1f-1** (ΔE_R = −4.9 kcal/mol) and **Tc1f-4** (ΔE_R = −4.2 kcal/mol) have activation barriers of >35 kcal/mol. None of the reactions shown in Fig. 8 should play a role in the thermal ethylene addition to **Tc1**.

The calculations thus predict that the technetium compound **Tc1** should react with ethylene in a different way than the rhenium compound **Re1**. The kinetically and thermodynamically most favorable pathway is the multi-step reaction with initial rearrangement **Tc1** → **Tc1a**, where the consecutive ethylene addition takes place yielding the dioxotechnetiumcyclopropane species **Tc1a-1**.

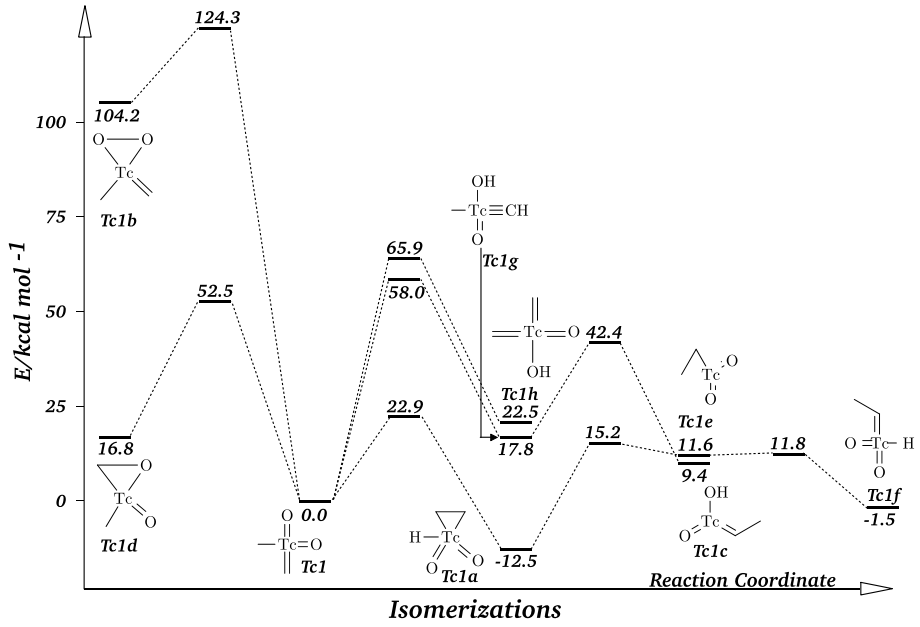

Fig. 5. Calculated reaction profile for the isomerizations of (O=)$_2$Tc(CH_3)(=CH_2) (**Tc1**) at B3LYP/II//B3LYP/I+ZPE.

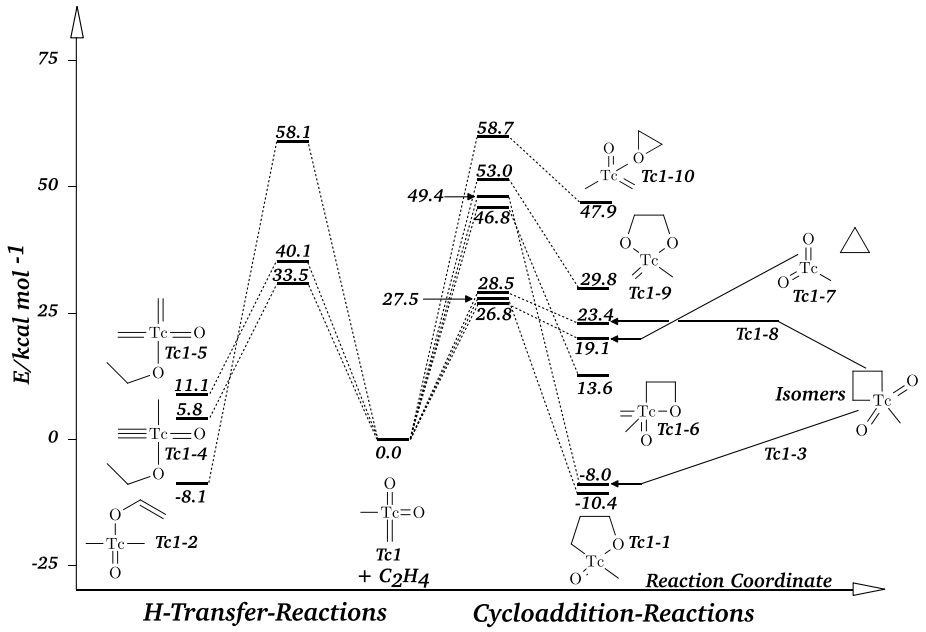

Fig. 6. Calculated reaction profile for the ethylene addition to $(O=)_2Tc(CH_3)(=CH_2)$ (**Tc1** + C_2H_4) at B3LYP/II//B3LYP/I+ZPE.

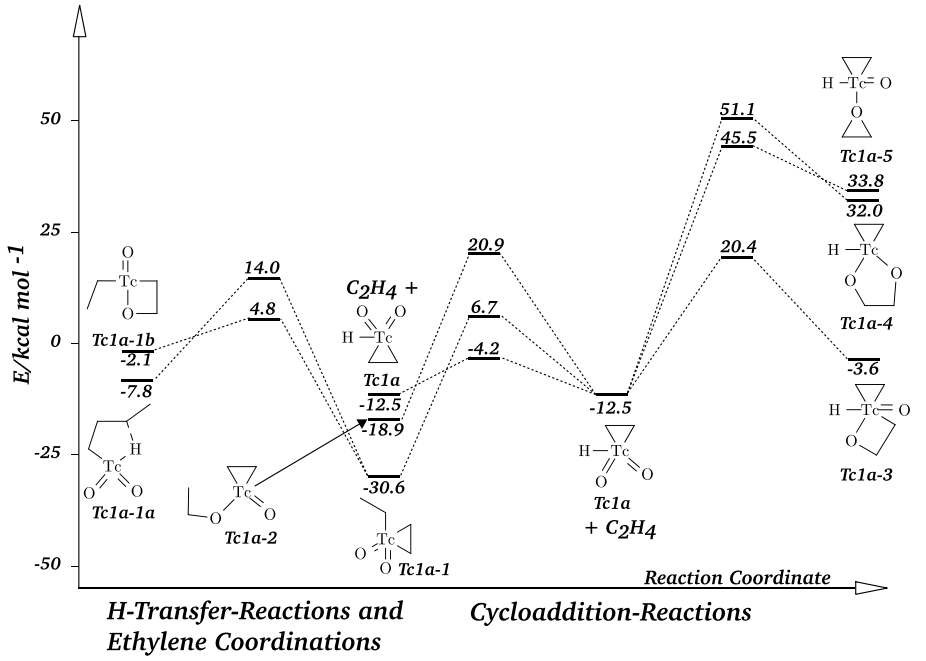

Fig. 7. Calculated reaction profile for the ethylene addition to $(O=)_2Tc(CH_2CH_2)(H)$ (**Tc1a** + C_2H_4) at B3LYP/II//B3LYP/I+ZPE.

The reaction has an overall barrier of 22.9 kcal/mol which comes from the rearrangement step and it is exothermic by 30.6 kcal/mol. Concerning the less favorable cycloaddition reactions of **Tc1** it is found that the $[3+2]_{C,O}$ reaction has a slightly lower barrier than the $[2+2]_{Tc,C}$ reaction and a much lower barrier than the $[2+2]_{Tc,O}$ reaction.

3.3. Reactions of $MnO_2(CH_3)(CH_2)$

Finally, we discuss the ethylene addition to **Mn1** which exhibits a higher complexity than the ethylene additions to the technetium and rhenium homologues. Elements of the first transition metal row often exhibit a different reactivity than their higher homologues of the second and third row. This is because the first d-shell of the atoms becomes filled with electrons which can therefore penetrate rather deeply into the core. It leads to a significantly different ratio of the 3d/4s radii of the valence orbitals compared with the 4d/5s and 5d/6s orbitals of the heavier elements [22].

Fig. 9 shows the calculated reaction profiles for the isomerization reactions of **Mn1**. Fig. 3S in Supplementary material displays the geometries of the most important energy minima and transition states of the manganese species. The exothermic rearrangement to the isomer **Mn1a'** which can be considered as ethylmangandioxide stabilized by agostic interactions has a very low activation barrier of only 4.3 kcal/mol. There is no rhenium and technetium analogue to the nonclassical structure of **Mn1a'**

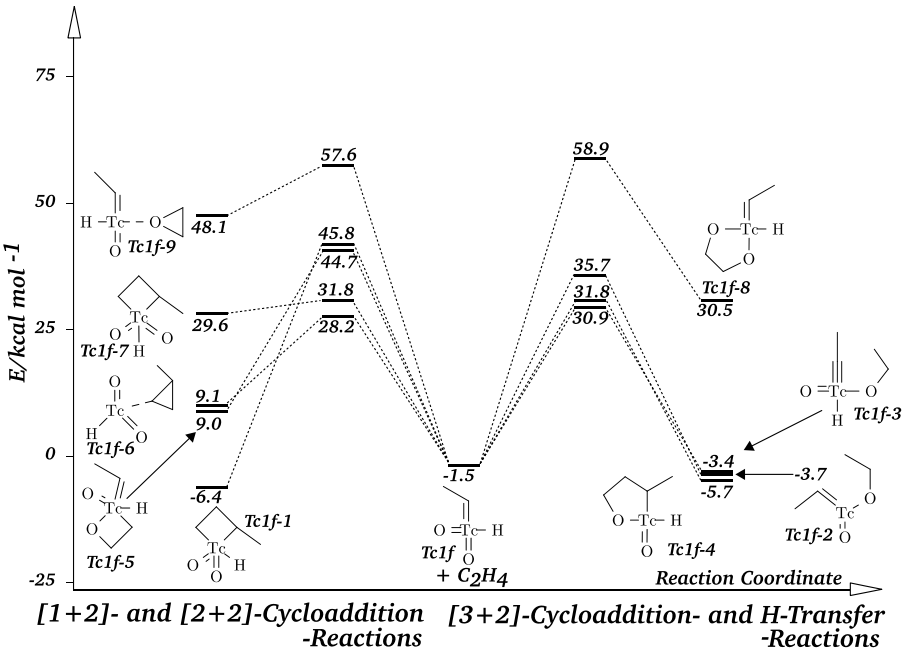

Fig. 8. Calculated reaction profile for the ethylene addition to $(O=)_2Tc(CHCH_3)(H)$ (**Tc1f** + C_2H_4) at B3LYP/II//B3LYP/I+ZPE.

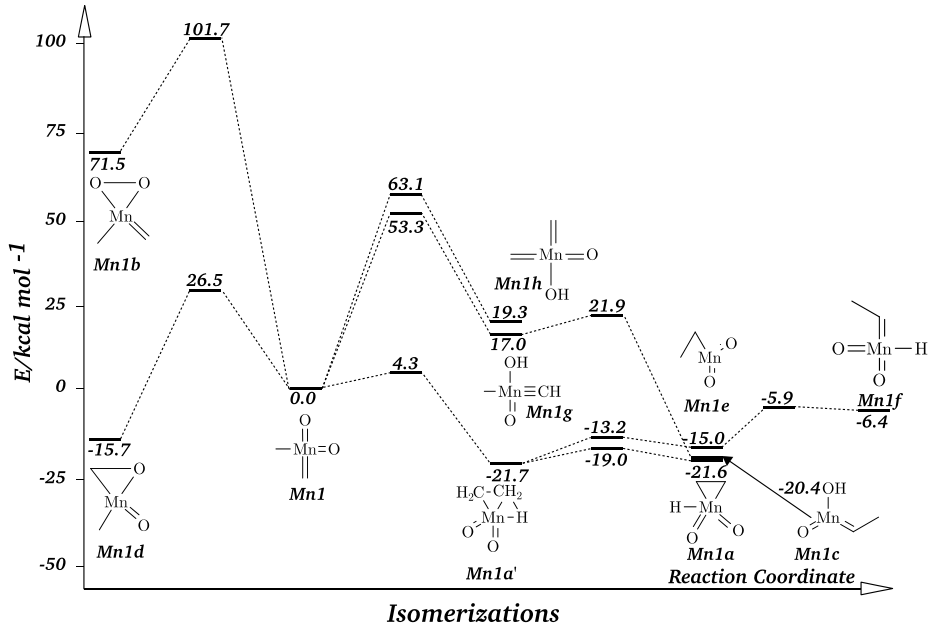

Fig. 9. Calculated reaction profile for the isomerizations of $(O=)_2Mn(CH_3)(=CH_2)$ (**Mn1**) at B3LYP/II//B3LYP/I+ZPE.

which further rearranges with a small barrier of 2.7 kcal/mol to the classical species **Mn1a**. The energetically nearly degenerate isomers **Mn1a'** and **Mn1a** are 21.7 and 21.6 kcal/mol lower in energy than **Mn1**. The activation energies for the other rearrangements are much higher lying and should not play a role in the thermal reactions. There is one more isomer **Mn1c** which is 20.4 kcal/mol more stable than **Mn1** but the kinetic barrier for its formation from **Mn1** is very high. Two other isomers **Mn1e** and **Mn1f** are lower in energy than **Mn1** and which are accessible from **Mn1a'** with comparatively low activation barriers (Fig. 9). Both species lie in very shallow potential wells and should therefore easily rearrange to the more stable isomer **Mn1a'**. Important structures which need to be considered for the reaction with ethylene are **Mn1**, **Mn1a'** and **Mn1a**.

Fig. 10 shows the reaction coordinates for ethylene addition to the parent manganese system **Mn1**. The kinetically most favorable reaction with an activation barrier of 8.1 kcal/mol is the [1 + 2] addition to the methylene group yielding cyclopropane and methylmanganesedioxide **Mn1-8**. There is a transition state between the latter product and the dioxometallacyclobutane compound **Mn1-1** which is formally the reaction product of the $[2 + 2]_{Mn,C}$ cycloaddition reaction. The IRC calculations showed, however, that **Mn1-1** is not accessible via the latter reaction but via addition of cyclopropane to $MeReO_2$. The $[3 + 2]_{C,O}$ addition leading to **Mn1-2** has a slightly higher barrier of 13.3 kcal/mol but it is much more exothermic (−38.0 kcal/mol) than the former reaction. The $[3 + 2]_{O,O}$ addition leading to **Mn1-9** has a much higher barrier (34.8 kcal/mol) and it is only slightly exothermic by 5.1 kcal/mol.

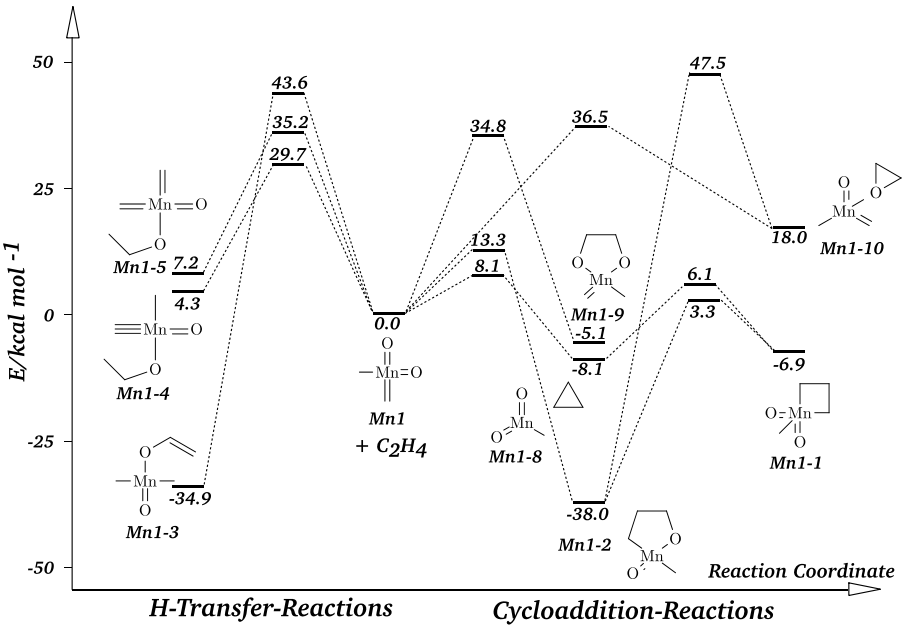

Fig. 10. Calculated reaction profile for the ethylene addition to $(O{=})_2Mn(CH_3)(=CH_2)$ (**Mn1** + C_2H_4) at B3LYP/II//B3LYP/I+ZPE.

Three addition reactions with concomitant hydrogen migration leading to **Mn1-3**, **Mn1-4** and **Mn1-5** have also very high activation barriers. Note that among the latter three reaction the only process which is strongly exothermic by −34.9 kcal/mol has the highest barrier (43.6 kcal/mol).

Since **Mn1** rearranges with a small barrier of only 4.3 kcal/mol to the more stable isomer **Mn1a'** (Fig. 9) it is pertinent to look for ethylene addition reactions to the latter structure. Fig. 11 shows the calculated reaction profiles. It becomes obvious that the ethylene addition to **Mn1a'** should easily proceed with a small barrier of 4.2 kcal/mol to the energetically low-lying product **Mn1a-1**. The transition state for the latter reaction (see Fig. S3 in Supplementary material) shows that the process takes place as a $[1 + 2]_{Mn}$ ethylene addition to the metal atom that requires very little energy. The overall reaction **Mn1** → **Mn1a'** (+C_2H_4) → **Mn1a-1** has an overall barrier of only 4.3 kcal/mol and it is exothermic by 39.4 kcal/mol. It should easily take place, although it does not lead to the most stable product which is rather the isomer **Mn1a-2** (Fig. 11). The addition reaction **Mn1a'** + C_2H_4 → **Mn1a-2** has a very high activation barrier of 46.3 kcal/mol which is strikingly higher than the thermodynamically less favored process **Mn1a'** + C_2H_4 → **Mn1a-1**. The results clearly show that the height of the transition state is not related to the thermodynamics of the reaction. Fig. 11 shows two other pathways for the addition of ethylene to **Mn1a'**, i.e. the $[3 + 2]_{O,O}$ addition and the addition to one oxygen atom with simultaneous migration of two hydrogen atoms. Both reactions have much higher barriers than the addition reaction yielding **Mn1a-1** and should therefore not play a role.

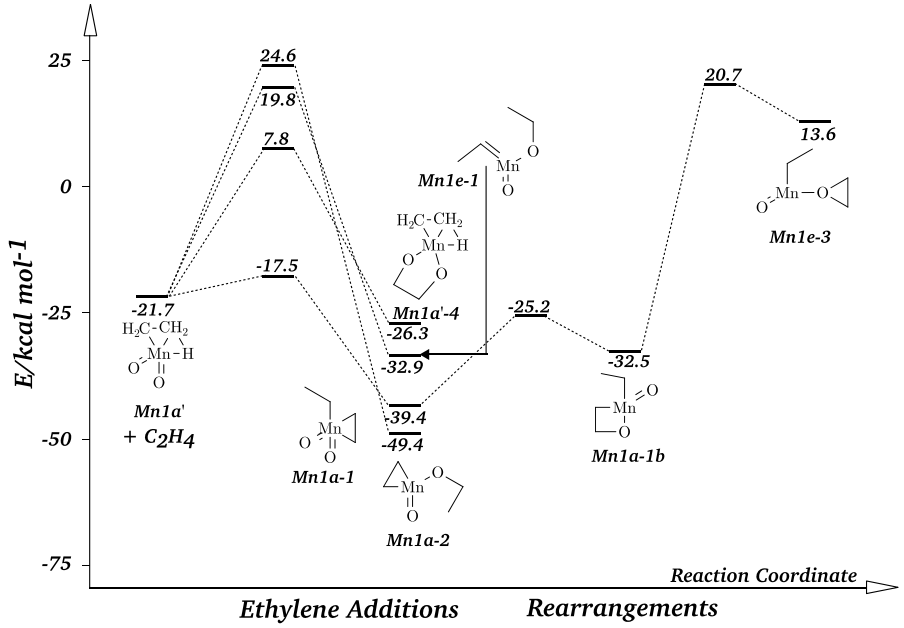

Fig. 11. Calculated reaction profile for the ethylene addition to $(O{=})_2Mn(CH_2CH_2H)$ (**Mn1a'** + C_2H_4) at B3LYP/II//B3LYP/I+ZPE.

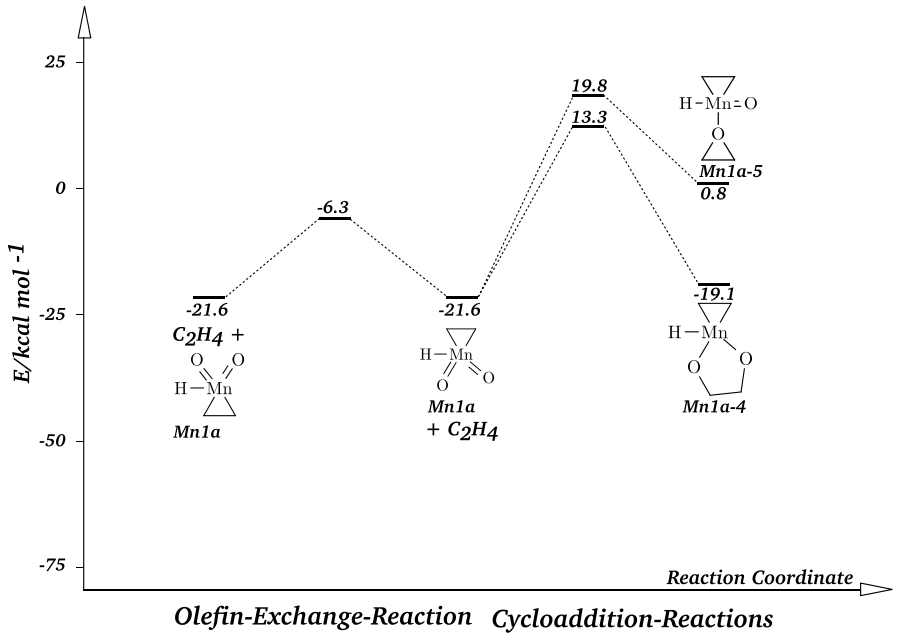

Fig. 12. Calculated reaction profile for the ethylene addition to $(O{=})_2Mn(CH_2CH_2)(H)$ (**Mn1a** + C_2H_4) at B3LYP/II//B3LYP/I+ZPE.

We calculated the reaction coordinates for ethylene addition to the shallow energy minima **Mn1e** and **Mn1f** in order to obtain a complete picture of the possible reaction pathways. The rather complex reactions which lead to altogether 13 different energy minima cannot compete with the above discussed low-energy pathways. Therefore they are not shown here. They are shown in Figs. S4 and S5 of Supplementary material. We do show in Fig. 12 the reaction profiles for ethylene addition to the isomer **Mn1a**, because the reactions of the heavier metals **Re1a** (Fig. 3) and **Tc1a** (Fig. 7) were important for the latter species. Fig. 12 shows that the activation barriers for the degenerate ethylene exchange (ΔE_A = 15.3 kcal/mol) and particularly for the $[3+2]_{O,O}$ addition yielding **Mn1a-4** (ΔE_A = 34.9 kcal/mol) and for the $[1+2]_O$ addition yielding **Mn1a-5** (ΔE_A = 41.4 kcal/mol) are too high to compete with the addition reaction of **Mn1a'**.

In summary, the reactions predict that the addition of ethylene to **Mn1** should rapidly take place with little activation energy as a two-step reaction with prior rearrangement to the more stable isomer **Mn1a'** and subsequent addition to the product molecule **Mn1a-1**.

3.4. Comparison of the group-7 elements

In order to directly compare the theoretically predicted reactivity of the group-7 compounds **M1** with ethylene we show in Fig. 13 the most favorable reaction pathway of the three elements.

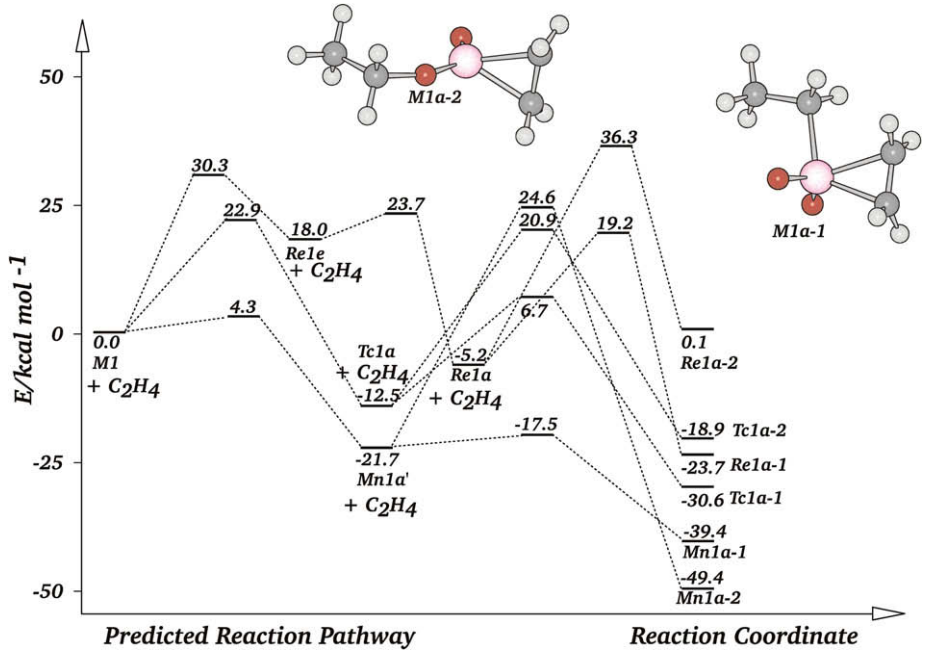

Fig. 13. Most favored reaction pathways for the ethylene addition to $(O{=})_2M(CH_3)(=CH_2)$ (M1 + C_2H_4) at B3LYP/II//B3LYP/I+ZPE.

The calculated activation barriers and reaction energies suggest the following reactivity order Mn > Tc > Re. Compound **Mn1** should easily rearrange to the more stable isomer **Mn1a'** which adds ethylene to the metal atom in an exothermic reaction yielding the metallacyclopropane compound **Mn1a-1** as product. The reaction product **Mn1a-2** is energetically lower lying than **Mn1a-1** but the activation barrier of 46.3 kcal/mol for the former product is much higher than for the latter species which has a barrier of only 4.3 kcal/mol. The energetically most favorable reactions of the heavier homologues **Tc1** and **Re1** with ethylene lead to the analogous products **Tc1a-1** and **Re1a-1** as the manganese compound but the reactions of the former elements are not only kinetically but also thermodynamically the most favored pathways (Fig. 13). The $[2+2]_{Re,C}$ cycloaddition reaction of **Re1** which is not shown in Fig. 13 has a slightly lower barrier of 27.7 kcal/mol but the reaction is endothermic by 22.4 kcal/mol. The calculations thus predict that for all metal systems **M1** the addition reaction with ethylene does neither follow a [3 + 2] nor a [2 + 2] pathway. The starting compounds rather first rearrange to dioxohydridometallacyclopropane species which react with ethylene with concomitant hydrogen migration. It can be expected that the molecules are not suitable for metathesis reactions.

It is illuminating to compare the calculated energy values for the activation barriers and reaction energies of the three metal systems **M1**. Table 1 gives the data for five isomerization processes while Table 2 shows the results for the addition reactions of ethylene. It becomes obvious that the rearrangements yielding the isomers **M1a**, **M1b** and **M1d** become clearly less favorable when the metal becomes heavier, i.e. the reactivity follows the order Mn > Tc > Re. All three reactions lead to a three-membered metallacyclic species (Figs. 1, 5 and 9). The same trend is observed for the hydrogen migration reactions leading to the isomers **M1g** and **M1h** but the differences are much smaller than for the former reactions (Table 1).

Table 2 shows that for most reaction pathways there is a reactivity trend Mn > Tc > Re which is predicted from the calculated activation barriers and reaction energies, i.e. the activation barrier in and the reaction energy becomes less exothermic or more endothermic when the metal becomes heavier. There are exceptions for the activation barriers of the formation of **M1-6** and **M1-7** for M = Tc, Re, where the latter metal has slightly smaller barriers than the former. Another exception is the multi-step formation of **M1a-2**, where the activation barrier of the manganese compound is much higher than for the technetium species.

4. Summary

The results of this work can be summarized as follows. The calculations suggest rather complex scenarios for the reaction of ethylene with the group-7 compounds $ReO_2(CH_3)(CH_2)$, $TcO_2(CH_3)(CH_2)$ and $MnO_2(CH_3)(CH_2)$. The $[2+2]_{Re,C}$ cycloaddition reaction of the starting molecule **Re1** is kinetically and thermodynamically favored over the $[3+2]_{C,O}$ and $[3+2]_{O,O}$ cycloadditions. However, the reaction which leads to the most stable product takes place with initial rearrangement to the dioxohydridometallacyclopropane isomer **Re1a** that adds ethylene with concomitant hydrogen migration yielding **Re1a-1**. The latter reaction has a slightly higher barrier than the $[2+2]_{Re,C}$ cycloaddition reaction. The direct $[3+2]_{C,O}$ cycloaddition becomes more favorable than the $[2+2]_{M,C}$ reaction for the starting compounds **Tc1** and **Mn1** of the lighter metals technetium and manganese but the calculations predict that other reactions are kinetically and thermodynamically more

Table 1
Calculated reaction energies (ΔE_R) and activation energies (ΔE_A) for the isomerization reactions of $(O=)_2Re(=CH_2)(CH_3)$ (**Re1**), $(O=)_2Tc(=CH_2)(CH_3)$ (**Tc1**) and $(O=)_2Mn(=CH_2)(CH_3)$ (**Mn1**) yielding the isomers **M1a**–**M1h** at B3LYP/II//B3LYP/I+ZPE

Product	$(O=)_2Mn(=CH_2)(CH_3)$ (**Mn1**)		$(O=)_2Tc(=CH_2)(CH_3)$ (**Tc1**)		$(O=)_2Re(=CH_2)(CH_3)$ (**Re1**)	
	ΔE_R	ΔE_A	ΔE_R	ΔE_A	ΔE_R	ΔE_A
M1a	−21.6	4.3[a]	−12.5	22.9	−5.2	30.3[b]
M1b	71.5	101.7	104.2	124.3	122.1	137.4
M1d	−15.7	26.5	16.8	52.5	34.9	68.4
M1g	17.0	53.3	17.8	58.0	22.9	60.9
M1h	19.3	63.1	22.5	65.9	26.7	66.9

All values are in kcal/mol.
[a] Highest barrier of a multi-step rearrangement with initial formation of **Mn1a'**.
[b] Highest barrier of a multi-step rearrangement with initial formation of **Re1e**.

Table 2
Calculated reaction energies (ΔE_R) and activation energies (ΔE_A) for selected additions of ethylene to $(O=)_2Re(=CH_2)(CH_3)$ (**Re1**), $(O=)_2Tc(=CH_2)(CH_3)$ (**Tc1**) and $(O=)_2Mn(=CH_2)(CH_3)$ (**Mn1**) at B3LYP/II//B3LYP/I+ZPE

Product	$(O=)_2Mn(=CH_2)(CH_3)_3$ (**Mn1**) + C_2H_4		$(O=)_2Tc(=CH_2)(CH_3)_3$ (**Tc1**) + C_2H_4		$(O=)_2Re(=CH_2)(CH_3)_3$ (**Re**) + C_2H_4	
	ΔE_R	ΔE_A	ΔE_R	ΔE_A	ΔE_R	ΔE_A
M1-1	−6.9	14.2[a]	−8.0	49.4	−6.8	48.9
M1-2	−38.0	13.3	−10.4	27.5	6.7	35.7
M1-6	–	–	13.6	46.8	16.3	44.0
M1-7	–	–	23.4	28.5	22.4	*27.7*
M1-8	−8.1	8.1	19.1	26.8	28.1	40.1
M1-9	−5.1	34.8	29.8	53.0	50.4	63.9
M1-10	18.0	36.5	47.9	58.7	67.2	76.8
M1a-1[a,b]	−39.4	*4.2*	*−30.6*	*22.9*	*−23.7*	30.3
M1a-2[b,c]	*−49.4*	46.3	−18.9	33.4	0.1	36.3

All values are in kcal/mol. The most favorable pathways are given in italics.
[a] Via a multi-step rearrangement where the highest barrier is given.
[b] The [1 + 2] addition to the metal takes place after multiple-step rearrangements **M1** + C_2H_4 → **M1a-1**.
[c] Ethylene addition to the terminal oxo group with concomitant hydrogen migration after multiple-step rearrangements **M1** + C_2H_4 → **M1a-2**.

favorable than the cycloadditions. The reactions with the lowest activation barriers lead after rearrangement to the ethyl substituted dioxometallacyclopropanes **Tc1a-1** and **Mn1a-1**. The manganese compound exhibits an even more complex reaction scenario than the technetium compounds. The thermodynamically most stable final product of ethylene addition to **Mn1** is the ethoxy substituted metallacyclopropane **Mn1a-2** which has, however, a high activation barrier.

Acknowledgements

This work was supported by the Deutsche Forschungsgemeinschaft. The generous allotment of computer time by the HRZ Marburg, the CSC Frankfurt and the HHLR Darmstadt are gratefully acknowledged.

Appendix A. Supplementary material

Cartesian coordinates of the optimized structures and the energies at B3LYP/I and B3LYP/II//B3LYP/I are available free of charge. Additionally, Figs. S1–S5 are given as Supplementary material. Supplementary data associated with this article can be found, in the online version, at doi:10.1016/j.jorganchem.2008.09.007.

References

[1] (a) U. Pidun, C. Boehme, G. Frenking, Angew. Chem. 108 (1996) 3008. Angew. Chem., Int. Ed. Engl. 35 (1996) 2817;
(b) S. Dapprich, G. Ujaque, F. Maseras, A. Lledós, D.G. Musaev, K. Morokuma, J. Am. Chem. Soc. 118 (1996) 11660;
(c) A.M. Torrent, L. Deng, M. Duran, M. Sola, T. Ziegler, Organometallics 16 (1997) 13;
(d) A.J. Del Monte, J. Haller, K.N. Houk, K.B. Sharpless, D.A. Singleton, T. Straßner, A.A. Thomas, J. Am. Chem. Soc. 119 (1997) 9907.
[2] (a) D.V. Deubel, G. Frenking, J. Am. Chem. Soc. 121 (1991) 2021;
(b) J. Frunzke, C. Loschen, G. Frenking, J. Am. Chem. Soc. 126 (2004) 3642;
(c) W.-P. Yip, W.Y. Yu, N. Zhu, C.-M. Che, J. Am. Chem. Soc. 127 (2005) 14239.
[3] Review: D.V. Deubel, G. Frenking, Acc. Chem. Res. 36 (2003) 645.
[4] D.V. Deubel, K. Muñiz, Chem. Eur. J. 10 (2004) 2475.
[5] M. Hölscher, W. Leitner, M.C. Holthausen, G. Frenking, Chem. Eur. J. 11 (2005) 4700.
[6] D. Cappel, S. Tüllmann, C. Loschen, M.C. Holthausen, G. Frenking, J. Organomet. Chem. 691 (2006) 4467. Note that the theoretical level of the calculations is slightly different from that in references 7,8 and also from that in the present work. Also, the transition states for the reactions **Os1** + ethylene → **Os3a** and **Os1** + ethylene → **Os3b** were only found after publication of this work. They are reported in Ref. 7.
[7] R. Haunschild, C. Loschen, S. Tüllmann, D. Cappel, M. Hölscher, M.C. Holthausen, G. Frenking, J. Phys. Org. Chem. 20 (2007) 11.
[8] R. Haunschild, G. Frenking, Z. Naturforsch. 62b (2007) 367.
[9] R. Haunschild, G. Frenking, J. Organomet. Chem. 693 (2007) 737.
[10] (a) A.D. Becke, J. Chem. Phys. 98 (1993) 5648;
(b) A.D. Becke, Phys. Rev. A 38 (1988) 3098;
(c) C. Lee, W. Yang, R.G. Parr, Phys. Rev. B 37 (1988) 785.
[11] P.J. Stephens, F.J. Devlin, G. Chabalowski, M.J. Frisch, J. Phys. Chem. 98 (1994) 11623.
[12] GAUSSIAN 03, Revision D.01, M.J. Frisch, G.W. Trucks, H.B. Schlegel, G.E. Scuseria, M.A. Robb, J.R. Cheeseman, J.A. Montgomery Jr., T. Vreven, K.N. Kudin, J.C. Burant, J.M. Millam, S.S. Iyengar, J. Tomasi, V. Barone, B. Mennucci, M. Cossi, G. Scalmani, N. Rega, G.A. Petersson, H. Nakatsuji, M. Hada, M. Ehara, K. Toyota, R. Fukuda, J. Hasegawa, M. Ishida, T. Nakajima, Y. Honda, O. Kitao, H. Nakai, M. Klene, X. Li, J.E. Knox, H.P. Hratchian, J.B. Cross, V. Bakken, C. Adamo, J. Jaramillo, R. Gomperts, R.E. Stratmann, O. Yazyev, A.J. Austin, R. Cammi, C. Pomelli, J.W. Ochterski, P.Y. Ayala, K. Morokuma, G.A. Voth, P. Salvador, J.J. Dannenberg, V.G. Zakrzewski, S. Dapprich, A.D. Daniels, M.C. Strain, O. Farkas, D.K. Malick, A.D. Rabuck, K. Raghavachari, J.B. Foresman, J.V. Ortiz, Q. Cui, A.G. Baboul, S. Clifford, J. Cioslowski, B.B. Stefanov, G. Liu, A. Liashenko, P. Piskorz, I. Komaromi, R.L. Martin, D.J. Fox, T. Keith, M.A. Al-Laham, C.Y. Peng, A. Nanayakkara, M. Challacombe, P.M.W. Gill, B. Johnson, W. Chen, M.W. Wong, C. Gonzalez, J.A. Pople, Gaussian, Inc., Wallingford CT, 2004.
[13] A. Schäfer, C. Huber, R. Ahlrichs, J. Chem. Phys. 100 (1994) 5829.
[14] D. Andrae, U. Häußermann, M. Dolg, H. Stoll, H. Preuß, Theor. Chim. Acta 77 (1990) 123.
[15] (a) M. Dolg, U. Wedig, H. Stoll, H. Preuss, J. Chem. Phys. 86 (1987) 866;
(b) S.P. Walch, C.W. Bauschlicher Jr., J. Chem. Phys. 78 (1983) 4597.
[16] (a) K. Fukui, J. Phys. Chem. 74 (1970) 4161;
(b) K. Fukui, Acc. Chem. Res. 14 (1981) 363.
[17] (a) J. Keck, Discuss. Faraday Soc. 33 (1962) 173;
(b) J.J.P. Stewart, L.P. Davis, L.W. Burggraf, J. Comp. Chem. 8 (1987) 1117;
(c) P.E. Blöchl, H.M. Senn, A. Togni, in: D.G. Truhlar, K. Morokuma (Eds.), Transition state modeling for catalysis, ACS Symposium Series, vol. 721, American Chemical Society, Washington, DC, 1999, pp. 88–99. ISBN-13: 978-0841236103.
[18] (a) R. Ahlrichs, M. Bär, M. Häser, H. Horn, C. Kölmel, Chem. Phys. Lett. 162 (1989) 165;
(b) O. Treutler, R. Ahlrichs, J. Chem. Phys. 102 (1995) 346.
[19] K. Eichkorn, F. Weigend, O. Treutler, R. Ahlrichs, Theor. Chem. Acc. 97 (1997) 119.
[20] T.H. Dunning, J. Chem. Phys. 90 (1989) 1007.
[21] J.M.L. Martin, A.J. Sundermann, J. Chem. Phys. 114 (2001) 3408.
[22] G. Frenking, N. Fröhlich, Chem. Rev. 100 (2000) 717.